RAPID COMMUNICATION

Superconductivity in Sm-doped $CaFe_2As_2$ single crystals*

Dong-Yun Chen(陈东云)[1], Bin-Bin Ruan(阮彬彬)[1], Jia Yu(于佳)[1], Qi Guo(郭琦)[1], Xiao-Chuan Wang(王小川)[1], Qing-Ge Mu(穆青隔)[1], Bo-Jin Pan(潘伯津)[1], Tong Liu(刘通)[1], Gen-Fu Chen(陈根富)[1,2], and Zhi-An Ren(任治安)[1,2,†]

[1] *Institute of Physics and Beijing National Laboratory for Condensed Matter Physics, Chinese Academy of Sciences, Beijing* 100190, *China*

[2] *Collaborative Innovation Center of Quantum Matter, Beijing* 100190, *China*

(Received 22 April 2016; revised manuscript received 26 April 2016; published online 20 May 2016)

In this article, the Sm-doping single crystals $Ca_{1-x}Sm_xFe_2As_2$ ($x = 0 \sim 0.2$) were prepared by the CaAs flux method, and followed by a rapid quenching treatment after the high temperature growth. The samples were characterized by structural, resistive, and magnetic measurements. The successful Sm-substitution was revealed by the reduction of the lattice parameter c, due to the smaller ionic radius of Sm^{3+} than Ca^{2+}. Superconductivity was observed in all samples with onset T_c varying from 27 K to 44 K upon Sm-doping. The coexistence of a collapsed phase transition and the superconducting transition was found for the lower Sm-doping samples. Zero resistivity and substantial superconducting volume fraction only happen in higher Sm-doping crystals with the nominal $x > 0.10$. The doping dependences of the c-axis length and onset T_c were summarized. The high-T_c observed in these quenched crystals may be attributed to simultaneous tuning of electron carriers doping and strain effect caused by lattice reduction of Sm-substitution.

Keywords: superconductivity, Sm-doping, $CaFe_2As_2$, collapsed structure

PACS: 74.70.Xa, 74.70.–b, 74.72.Ek **DOI:** 10.1088/1674-1056/25/6/067403

1. Introduction

Among the iron-based high-T_c superconductors, the 122-type ternary compounds AFe_2As_2 (A = Ca, Sr, Ba, and Eu) crystallize in the tetragonal $ThCr_2Si_2$-type crystal structure at room temperature, and they undergo a spin density wave (SDW) transition around 140 K $\sim$ 200 K, which is also accompanied by a structural transition from tetragonal to orthorhombic phase at similar temperature.[1–5] Bulk superconductivity was achieved in these compounds by suppressing the antiferromagnetic SDW ordering via hole or electron doping, even external pressure, etc., and their superconducting T_c is usually below 38 K.[6–11]

While interestingly, unexpected high-T_c above 40 K was realized in some rare-earth-doped $Ca_{1-x}R_xFe_2As_2$ compounds (R = La, Ce, Pr, and Nd), with the highest T_c up to 49 K in Pr-doped $CaFe_2As_2$.[12–16] This higher T_c phase in electron doped $CaFe_2As_2$ is usually filament type with poor superconducting behaviors and highly anisotropic characteristics.[12,13,15,17,18] Some possible reasons were proposed to explain the occurrence of this higher T_c phase, such as crystallographic strain, doping inhomogeneity, and crystal defects, etc.[13,19–23] On the other hand, $CaFe_2As_2$ is actually special in these 122 compounds, it has the shortest c-axis parameter and the smallest cell volume, which places it near the critical point for a unique collapsed structural phase transition.[9,12,24–32] Generally, the pristine tetragonal $CaFe_2As_2$ enters into the orthorhombic SDW phase around 170 K, while under a mild external pressure of 0.35 GPa, a collapsed, non-magnetic tetragonal phase would be formed at lower temperature without the formation of SDW phase.[24,25] This collapsed phase can also be stabilized by chemical substitution or furnace quenching processes.[9,12,26–30] Moreover, La and P co-doping in $CaFe_2As_2$ enhances both the superconducting transition temperature and the shielding volume fraction, which is suggested to be from the simultaneous tuning of the reduction in cell volume and the electron carrier doping.[33] Similar results occur in the La and Ru co-doped $CaFe_2As_2$ single crystals.[27] Due to the smaller ionic radius of Sm^{3+} than Ca^{2+}, the substitution of Sm^{3+} for Ca^{2+} may be a suitable method for the structure and carrier modulation in $CaFe_2As_2$. While the doping of Sm^{3+} for Ca^{2+} is experimentally difficult due to structural instability, and previous study found no clear superconductivity in slightly Sm-doping $CaFe_2As_2$ single crystals grown from FeAs flux.[34]

In this article, we report the successful growth of the Sm-doped $CaFe_2As_2$ single crystals from CaAs flux. Superconductivity with T_c varying from 27 K to 44 K was observed in these crystals, with a relatively substantial shielding volume fraction obtained in the nominal $Ca_{0.8}Sm_{0.2}Fe_2As_2$ single crystal.

*Project supported by the National Natural Science Foundation of China (Grant No. 11474339), the National Basic Research Program of China (Grant Nos. 2010CB923000 and 2011CBA00100), and the Strategic Priority Research Program of the Chinese Academy of Sciences (Grant No. XDB07020100).

†Corresponding author. E-mail: renzhian@iphy.ac.cn

© 2016 Chinese Physical Society and IOP Publishing Ltd

2. Experimental details

Single crystals of $Ca_{1-x}Sm_xFe_2As_2$, with $x = 0$, 0.01, 0.02, 0.03, 0.05, 0.10, 0.15, 0.20, were grown using the CaAs flux method. A mixture of Ca, Sm, FeAs, and As with a mole ratio of Ca:Sm:FeAs:As = $(3-3x)$:$3x$:2:2 was loaded into an alumina crucible and sealed in an evacuated quartz tube. The ampoules were placed in a muffle furnace and heated at 500 °C and 700 °C for 5 h successively, then slowly heated to 1150 °C for 10 h, maintained at 1150 °C for 30 h and then cooled down to 850 °C slowly at a rate of 1.5 °C/h, followed by quenching in ice-water rapidly. Plate-like single crystals up to 1-mm long were obtained after the flux was removed by washing the products in de-ionized water. The FeAs precursor was pre-sintered by reacting stoichiometric amounts of Fe and As inside an evacuated quartz tube at 750 °C for 30 h.

The obtained plate-like single crystals were characterized by x-ray diffraction (XRD) from 10° to 70° at room temperature, using a PAN-analytical diffractometer with Cu–K_α radiation. The resistive measurements were carried out by employing a standard four-probe method in a quantum design physical property measurement system (PPMS) down to 2 K. The DC magnetic susceptibility was measured using a quantum design magnetic property measurement system (MPMS) with both zero field cooling (ZFC) and field cooling (FC) methods at a magnetic field of 10 Oe (1 Oe = 79.5775 A/m).

3. Results and discussion

The room temperature XRD patterns for all the single crystals of $Ca_{1-x}Sm_xFe_2As_2$ samples were presented in Fig. 1 with an enlarged view around (008) reflections placed on the right panel, and an image of a typical plate-like $Ca_{0.85}Sm_{0.15}Fe_2As_2$ single crystal was also displayed in the inset. We note that for the Sm-doped $CaFe_2As_2$, the crystal growth is difficult, and the crystal size is usually less than 1 mm and much smaller than the undoped crystal. The observation for the (00l) reflections indicates preferential orientation of the single crystals along the c-axis and good crystal quality. As shown from the enlarged view of (008) peaks, we see that the (008) peak moves to higher diffraction angle with the increasing of Sm-doping level when $x < 0.10$. After $x > 0.10$ no obvious change of the peak position was observed, which indicates that the real Sm-doping level nearly reaches a maximum when the nominal Sm concentration $x > 0.10$. The c-axis parameter was calculated and plotted as a function of the nominal Sm concentration x in Fig. 5(a). The reduction of the c-axis parameter with increasing x indicates that Sm is a successful substitution for Ca, since the trivalent Sm^{3+} (0.96 Å) has a smaller ionic radius than the divalent Ca^{2+} (0.99 Å). Comparing with other rare-earth doped $CaFe_2As_2$, the Sm-doped crystal has much shorter c-axis length,[12] which may cause strong chemical pressure on the Fe–As plane. We note that for the quenched undoped $CaFe_2As_2$, the c-axis parameter is much smaller than that of the pristine $CaFe_2As_2$ parent compound,[4] and the dramatic c-axis shrinkage is due to the effect of strong internal crystallographic strain induced by the quenching process.[26,35]

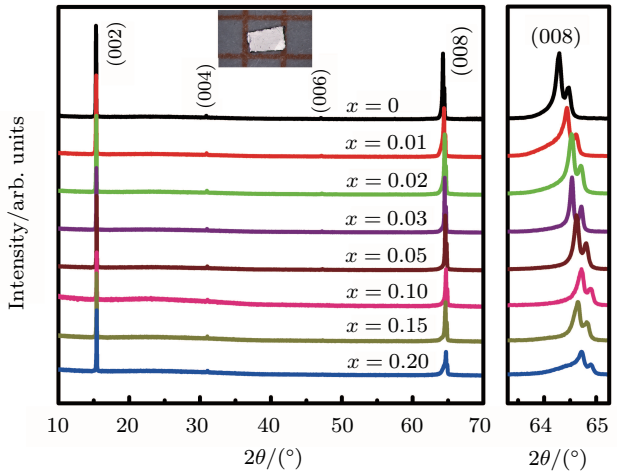


Fig. 1. (color online) The room temperature XRD patterns for the $Ca_{1-x}Sm_xFe_2As_2$ ($x = 0 \sim 0.2$) single crystals, with an expanded view near the (008) peaks placed in the right panel. The inset displays an image of a typical plate-like $Ca_{0.85}Sm_{0.15}Fe_2As_2$ single crystal.

In Fig. 2 we present the temperature dependence of the normalized in-plane electric resistivity for all of the $Ca_{1-x}Sm_xFe_2As_2$ single crystals measured between 2 K to 300 K. We observed strain caused superconductivity at 27 K in the undoped quenched $CaFe_2As_2$ crystal, which was discussed in another paper.[35] As shown in Fig. 2(a), all the lower doping samples ($x < 0.05$) display weak superconductivity with the onset T_c increasing monotonically upon Sm doping, from 27 K for undoped samples to 43 K for sample with $x = 0.03$, and two step superconducting transitions were observed in these crystals. No zero resistivity was found in these lower doping crystals. Besides the superconducting transition, all these lower doping samples show another transition characterized by a resistive drop around 70 K–110 K. The resistivity drop in rare-earth doped or pristine $CaFe_2As_2$ single crystal around this temperature range is a typical indication for the collapsed structural phase transition as previously reported.[12,36] This means the existence of filament type superconductivity in the collapsed phase. For higher doping samples with $x \geq 0.05$ as displayed in Fig. 2(b), this structural transition induced resistive drop disappears, which should be suppressed by the higher level Sm-doping. This is consistent with the previous report that more electron doping counteracts the chemical pressure which induces the collapsed phase transition.[27] The changing of this collapsed phase transition still needs to be further verified by low temperature structural characterizations. The superconducting transition for these higher doping crystals becomes much sharper, with the onset T_c all close to 44 K. When $x \geq 0.10$, the resistive curves

become very similar, and zero resistivity was observed around 30 K in these samples. The relationship for onset T_c versus Sm-doping level x was summarized in Fig. 5(b).

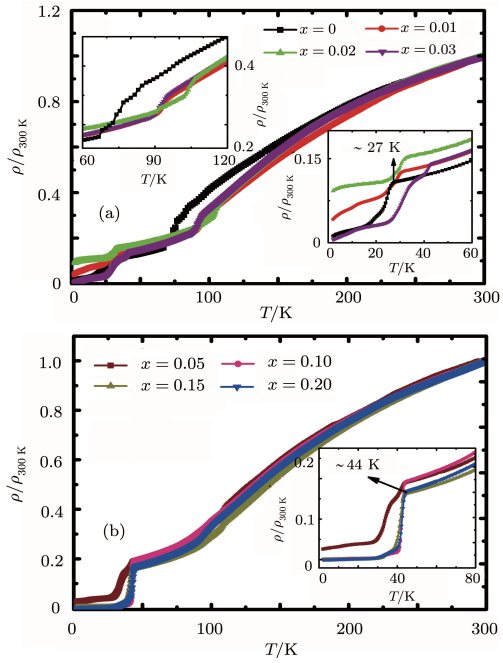


Fig. 2. (color online) The temperature dependence of normalized in-plane resistivity for $Ca_{1-x}Sm_xFe_2As_2$ single crystals of (a) lower doping samples ($x = 0.00, 0.01, 0.02, 0.03$) and (b) higher doping samples ($x = 0.05, 0.10, 0.15, 0.20$). The insets show the expanded resistive curves around the collapsed phase transition and the superconducting transition respectively.

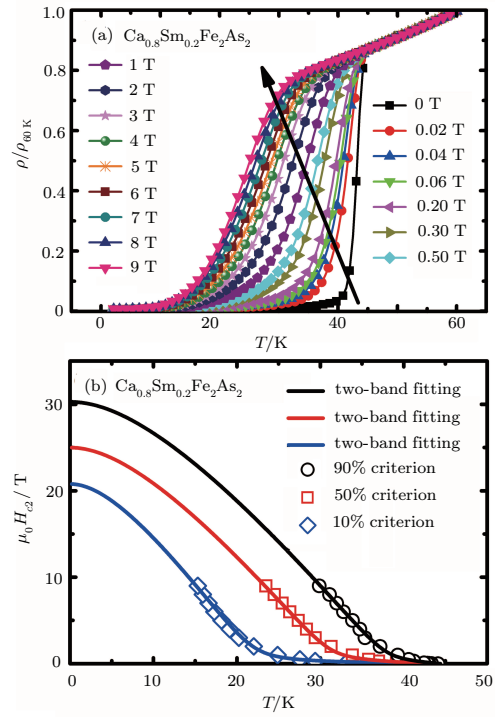


Fig. 3. (color online) (a) The temperature dependence of normalized resistivity between 2 K and 60 K under different magnetic fields for a $Ca_{0.8}Sm_{0.2}Fe_2As_2$ single crystal. (b) The upper critical field $\mu_0 H_{c2}$ determined by resistive curves with three different criteria: 90%, 50%, and 10% of normal state resistivity, and the solid lines represent the fitting results with two-band model.

To estimate the upper critical field, the resistive superconducting transition for a $Ca_{0.8}Sm_{0.2}Fe_2As_2$ single crystal was characterized between 2 K and 60 K under magnetic fields of 0 T$\sim$9 T applied along the c axis, as shown in Fig. 3(a). With increasing magnetic field, the transition temperature decreases, and the transition width increases, while zero resistivity still survives at the maximal field of 9 T. The upper critical field $\mu_0 H_{c2}(T)$ was calculated using three different criteria of 90%, 50%, 10% of the normal state resistivity, which is presented in Fig. 3(b). The temperature dependence of $\mu_0 H_{c2}(T)$ curves from different criteria all show remarkable upward curvatures near T_c, and we accordingly fit the curves by the two-band theory.[37] The two-band fits agree well with the $\mu_0 H_{c2}(T)$ data and give values of $\mu_0 H_{c2}(0)$ at different criteria about 30.3 T, 25.0 T, and 20.8 T, respectively.

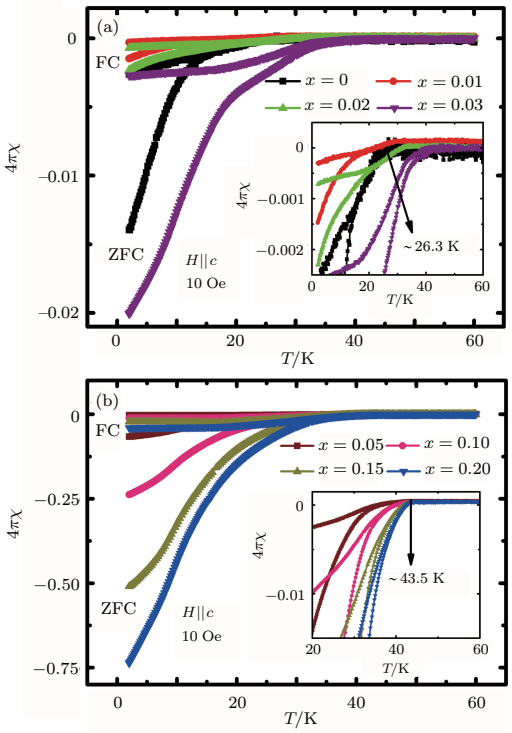


Fig. 4. (color online) The temperature dependence of DC magnetic susceptibility with both ZFC and FC measurements for the $Ca_{1-x}Sm_xFe_2As_2$ single crystals ($x = 0.00, 0.01, 0.02, 0.03$ in panel (a) and $x = 0.05, 0.10, 0.15, 0.20$ in panel (b)). The insets show the enlarged view around the superconducting transition.

In Fig. 4 we presented the temperature dependence of DC magnetic susceptibility for all the samples, which was measured between 2 K and 60 K with both zero-field-cooling (ZFC) and field-cooling (FC) methods under a magnetic field of 10 Oe. Consistent with the resistivity results, all the samples display superconducting Meissner transition, and the onset T_c changes from 26.3 K for $x = 0.00$ to 43.5 K for $x = 0.20$, which is slightly lower than that determined by the resistive measurements. For the lower doping samples in Fig. 4(a), the onset T_c increases with the doping level x, while the diamagnetic signal is very weak, which indicates the very low superconducting volume fraction of filament type. For the higher doping samples in Fig. 4(b), the onset T_c becomes very close for all samples, while the superconducting shielding volume fraction increases quickly with the nominal Sm concentration

x, which suggests that tiny increase of the Sm-doping level still improves the formation of superconducting phases.

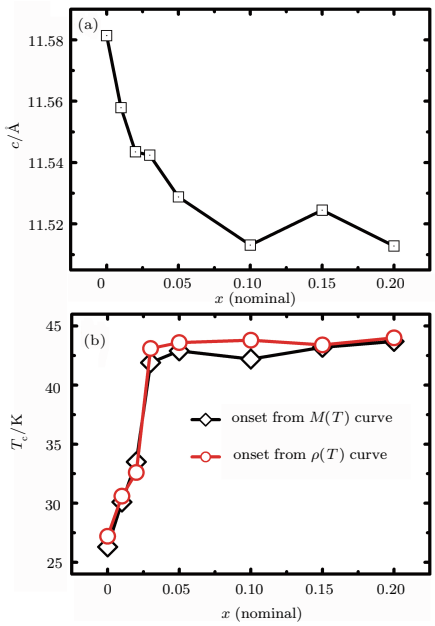


Fig. 5. (color online) The relationship between the nominal Sm-doping concentration x and (a)c-axis parameter, (b) onset T_c determined by resistive and magnetic measurements for all the $Ca_{1-x}Sm_xFe_2As_2$ single crystals.

In Fig. 5, we summarized the relationship for the lattice parameter c and the onset T_c versus the nominal Sm-doping concentration x. The c-axis length decreases monotonically with increasing x when $x < 0.05$, and accordingly, the onset T_c increases to the maximum around 44 K. And after $x > 0.05$, the lattice parameter c becomes almost constant, and the onset T_c show no clear change around 44 K. All these results exhibit that Sm is a successful dopant for $CaFe_2As_2$ compound, and it produces high-T_c up to 44 K in the nominal $Ca_{0.8}Sm_{0.2}Fe_2As_2$ single crystal with substantial superconducting volume fraction, which may be attributed to the simultaneous tuning of electron carriers doping and strain effect caused by lattice reduction.

In conclusion, we successfully grew the single crystals of $Ca_{1-x}Sm_xFe_2As_2$ ($x = 0.00 \sim 0.20$) using a CaAs flux method followed by a rapid quenching process. The Sm-doping was elucidated by the reduction of c-axis parameter with increasing x, and superconductivity was observed in all the Sm-doped crystals. High-T_c superconductivity up to 44 K was proved by both the resistive and magnetic measurements in the Sm-doped $CaFe_2As_2$ single crystals.

References

[1] Howard C J and Carpenter M A 2012 *Acta Crystallogr. B* **68** 209
[2] Jiang H, Sun Y L, Xu Z A and Cao G H 2013 *Chin. Phys. B* **22** 087410
[3] Ni N, Nandi S, Kreyssig A, Goldman A I, Mun E D, Bud'ko S L and Canfield P C 2008 *Phys. Rev. B* **78** 014523
[4] Goldman A I, Argyriou D N, Ouladdiaf B, Chatterji T, Kreyssig A, Nandi S, Ni N, Bud'ko S L, Canfield P C and McQueeney R J 2008 *Phys. Rev. B* **78** 100506
[5] Ren Z A, Lu W, Yang J, Yi W, Shen X L, Li Z C, Che G C, Dong X L, Sun L L, Zhou F and Zhao Z X 2008 *Chin. Phys. Lett.* **25** 2215
[6] Matsubayashi K, Katayama N, Ohgushi K, Yamada A, Munakata K, Matsumoto T and Uwatoko Y 2009 *J. Phys. Soc. Jpn.* **78** 073706
[7] Li Z C, Lu W, Dong X L, Zhou F and Zhao Z X 2010 *Chin. Phys. B* **19** 026103
[8] Zhao K, Liu Q Q, Wang X C, Deng Z, Lv Y X, Zhu J L, Li F Y and Jin C Q 2010 *J. Phys.: Condens. Matter* **22** 222203
[9] Wang D M, Shangguan X C, He J B, Zhao L X, Long Y J, Wang P P and Wang L 2013 *J. Supercond. Novel Magn.* **26** 2121
[10] Kasahara S, Shibauchi T, Hashimoto K, Nakai Y, Ikeda H, Terashima T and Matsuda Y 2011 *Phys. Rev. B* **83** 060505
[11] Rotter M, Tegel M and Johrendt D 2008 *Phys. Rev. Lett.* **101** 107006
[12] Saha S R, Butch N P, Drye T, Magill J, Ziemak S, Kirshenbaum K, Zavalij P Y, Lynn J W and Paglione J 2012 *Phys. Rev. B* **85** 024525
[13] Lv B, Deng L, Gooch M, Wei F, Sun Y, Meen J K, Xue Y Y, Lorenz B and Chu C W 2011 *Proc. Natl. Acad. Sci. USA* **108** 15705
[14] Gao Z, Qi Y, Wang L, Wang D, Zhang X, Yao C, Wang C and Ma Y 2011 *Europhys. Lett.* **95** 67002
[15] Qi Y, Gao Z, Wang L, Wang D, Zhang X, Yao C, Wang C, Wang C and Ma Y 2012 *Supercond. Sci. Technol.* **25** 045007
[16] Ying J J, Liang J C, Luo X G, Wang X F, Yan Y J, Zhang M, Wang A F, Xiang Z J, Ye G J, Cheng P and Chen X H 2012 *Phys. Rev. B* **85** 144514
[17] Zhou W, Yuan F F, Zhuang J C, Sun Y, Ding Y, Cui L J, Bai J and Shi Z X 2013 *Supercond. Sci. Technol.* **26** 095003
[18] Huang Y B, Richard P, Wang J H, Wang X P, Shi X, Xu N, Wu Z, Li A, Yin J X, Qian T, Lv B, Chu C W, Pan S H, Shi M and Ding H 2013 *Chin. Phys. Lett.* **30** 017402
[19] Sun Y, Zhou W, Cui L J, Zhuang J C, Ding Y, Yuan F F, Bai J and Shi Z X 2013 *AIP Adv.* **3** 102120
[20] Chu C W, Lv B, Deng L Z, Lorenz B, Jawdat B, Gooch M, Shrestha K, Zhao K, Zhu X Y, Xue Y Y and Wei F Y 2013 *J. Phys: Conf. Ser.* **449** 012014
[21] Tamegai T, Ding Q P, Ishibashi T and Nakajima Y 2013 *Physica C* **484** 31
[22] Gofryk K, Pan M, Cantoni C, Saparov B, Mitchell J E and Sefat A S 2014 *Phys. Rev. Lett.* **112** 047005
[23] Deng L Z, Lv B, Zhao K, Wei F Y, Xue Y Y, Wu Z and Chu C W 2016 *Phys. Rev. B* **93** 054513
[24] Torikachvili M S, Bud'ko S L, Ni N and Canfield P C 2008 *Phys. Rev. Lett.* **101** 057006
[25] Kreyssig A, Green M A, Lee Y, Samolyuk G D, Zajdel P, Lynn J W, Bud'ko S L, Torikachvili M S, Ni N, Nandi S, Leão J B, Poulton S J, Argyriou D N, Harmon B N, McQueeney R J, Canfield P C and Goldman A I 2008 *Phys. Rev. B* **78** 184517
[26] Ran S, Bud'ko S L, Pratt D K, Kreyssig A, Kim M G, Kramer M J, Ryan D H, Rowan-Weetaluktuk W N, Furukawa Y, Roy B, Goldman A I and Canfield P C 2011 *Phys. Rev. B* **83** 144517
[27] Zhao K, Stingl C, Manna R S, Jin C Q and Gegenwart P 2015 *Phys. Rev. B* **92** 235132
[28] Danura M, Kudo K, Oshiro Y, Araki S, C. Kobayashi T and Nohara M 2011 *J. Phys. Soc. Jpn.* **80** 103701
[29] Ma L, Ji G F, Dai J, Saha S R, Drye T, Paglione J and Yu W Q 2013 *Chin. Phys. B* **22** 057401
[30] Yang R, Le C, Zhang L, Xu B, Zhang W, Nadeem K, Xiao H, Hu J and Qiu X 2015 *Phys. Rev. B* **91** 224507
[31] Saha S R, Drye T, Goh S K, Klintberg L E, Silver J M, Grosche F M, Sutherland M, Munsie T J S, Luke G M, Pratt D K, Lynn J W and Paglione J 2014 *Phys. Rev. B* **89** 134516
[32] Xu D F, Shen D W, Jiang J, Ye Z R, Liu X, Niu X H, Xu H C, Yan Y J, Zhang T, Xie B P and Feng D L 2014 *Phys. Rev. B* **90** 214519
[33] Kudo K, Iba K, Takasuga M, Kitahama Y, Matsumura J, Danura M, Nogami Y and Nohara M 2013 *Sci. Rep.* **3** 1478
[34] Wei F, Lv B, Deng L, Meen J K, Xue Y Y and Chu C W 2014 *Philos. Mag.* **94** 2562
[35] Chen D Y, Yu J, Ruan B B, Guo Q, Zhang L, Mu Q G, Wang X C, Pan B J, Chen G F and Ren Z A 2016 arXiv: 1604.04964
[36] Gao B, Li X, Ji Q, Mu G, Li W, Hu T, Li A and Xie X 2014 *New J. Phys.* **16** 113024
[37] Gurevich A 2003 *Phys. Rev. B* **67** 184515